Fatigue crack growth in complex tubular joints

Fatigue Crack Growth in Complex Tubular Joints

Propagation de fissures de fatigue dans des joints tubulaires complexes

Ermüdungsrisswachstum in komplexen Verbindungen von Rohrprofilen

Björn SKALLERUD
Research Eng.
SINTEF
Trondheim, Norway

Björn Skallerud, born 1959, received his master of engineering and doctoral degrees at the Norwegian Inst. of Technology. He has been working with problems related to cyclic plasticity and low and high cycle fatigue.

Oddvar I. EIDE
Senior Research Eng.
SINTEF
Trondheim, Norway

Oddvar I. Eide, born 1951, obtained his master of engineering degree at the Norwegian Inst. of Technology. He is performing research in fatigue and fracture of welded structures, in this area he also holds a doctoral degree.

Stig BERGE
Professor
Norw. Inst. of Techn.
Trondheim, Norway

Stig Berge, born 1942, received his master of engineering and doctoral degrees at the Norwegian Inst. of Technology. He is a professor at the Division of Marine Structures, where he teaches and carries out research in the area of fatigue and fracture of offshore structures.

SUMMARY
Fatigue crack growth data from tests of stiffened tubular joints are reported. Fracture mechanics models for part through and through crack growth analysis are presented, and these results are compared with experimental data.

RÉSUMÉ
Des résultats de propagation de fissures de fatigue provenant d'essais sur des joints de tubes raidis sont présentés. D'autre part, des modèles de la mécanique de la rupture pour la propagation de fissures à travers l'épaisseur de la pièce sont également présentés, et ces résultats sont comparés avec les valeurs expérimentales.

ZUSAMMENFASSUNG
Berichtet wird über Resultate aus Versuchen an ausgesteiften Verbindungen röhrenförmiger Profile. Bruchmechanische Modelle zur Analyse des Wachstums durchgehender und nichtdurchgehender Risse werden vorgestellt. Die Resultate dieser Analysen werden mit denjenigen der Versuche verglichen.

1. INTRODUCTION

One common type of stiffened tubular joints is the connection between a brace and a comparatively much larger chord, like brace column or brace/pontoon connections of semi-submersible rigs. These connections are based on load transfer through internal stiffening of the brace into an array of stiffened deck and bulkhead details in the column or pontoon. Due to the complicated geometry, it is difficult to calculate the stress flow through structural details of this type, and in particular to assess realistic stress concentration factors for the various weld details. Service experience has proved these joints to be fatigue vulnerable. Similar type of joints may also be used in deep water jacket structures, in which fatigue damage may become very critical due to the general problems of detection and repair at great waterdepths.

With the development of fracture mechanics, methods have become available for calculation of the significance of defects, residual life of cracked structures etc., which are required in order to establish rational criteria for inspection, maintenance, and repair procedures. Furthermore, fracture mechanics has proved to be a useful tool in the analysis of fatigue test data, enabling conclusions to be drawn on the basis of physical models rather than statistical analysis of S-N data.

Within a recent research program, fatigue behaviour of simplified but realistic models of brace/column connections has been studied. The aims of the investigation were to provide S-N data for this type of structural details. Furthermore, to investigate crack growth behaviour in this type of joints in order to establish and verify fracture mechanics models for assessment of residual life and consequences of cracking if detected. S-N data obtained with the brace/column models are reported elsewhere [1]. The emphasis in the present paper is on fracture mechanics modelling and analysis of fatigue crack growth.

2. EXPERIMENTAL INVESTIGATION

2.1 Specimen and loading

The specimens were simplified but realistic models of brace/column connections with internal stiffening. The main dimensions are shown in Fig. 1. The models were constructed such that two connections could be tested simultaneously. The brace dimensions were 711 mm outer diameter and 12.5 mm plate thickness. Due to the comparatively much larger column dimensions for this type of joints, the column was modelled by plane plates. Two models were produced. In order to investigate the effects of external stiffeners on fatigue behaviour of the present type of joints, one of the models was tested with external gussets at the brace/column intersection, cf. Fig. 1.

The brace material was spiral welded tube made from structural steel to NVE-36. The spiral welds were ground flush prior to specimen fabrication. The plate material was a structural steel to St52-3. The yield strengths were in the range 360-400 MPa.

The models were produced by manual metal arc welding, using basic electrodes. All welds were made as fillet welds. Nominal weld throat was 40 per cent of the plate thickness. The weld details at the end of the internal stiffening in the brace (Position 3 in Fig. 1) were post weld treated by grinding. All other welds were in the as-welded condition.

Testing was performed in constant amplitude axial loading using a 2 MN dynamic actuator. The test rig arrangement is shown in Fig. 2. Nominal stress in the braces were measured by strain gauges attached 300 mm from the brace end and spaced 90 degrees around the brace circumference. No global bending of the braces was observed. Measured stresses were within the range 1.0-1.1 of the computed nominal stress in the brace, the stress enhancement being interpreted as effects of local cross sectional imperfections.

During testing, fatigue cracks developed at the brace/column welds (Pos. 1) and at the ends of external gusset (Pos. 2) and internal stiffener (Pos. 3). The welds were periodically checked for crack initiation by spraying white spirit on the surface during testing. Fatigue cracks were then clearly visible by the pumping of liquid in and out of the crack. When cracks were detected, through thickness crack growth was monitored by a high-frequency, alternating current potential drop system. Surface crack lengths were obtained by visual measurements, using white spirit. Fracture surface examinations showed that the use of white spirit also deposited beachmarks at the fracture surfaces. At the end of testing, crack growth data was checked against the surface markings, providing a direct calibration.

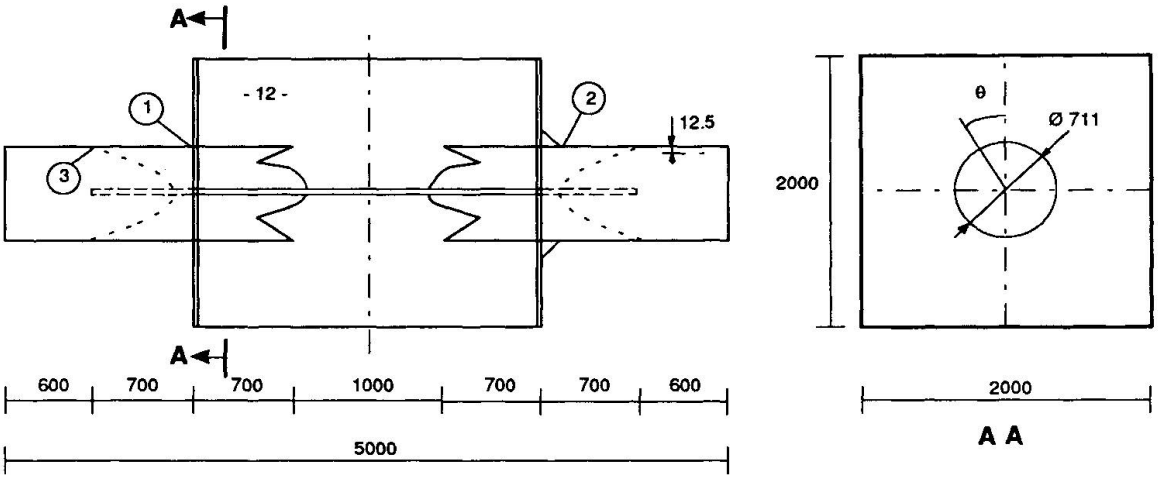

Figure 1 Specimen

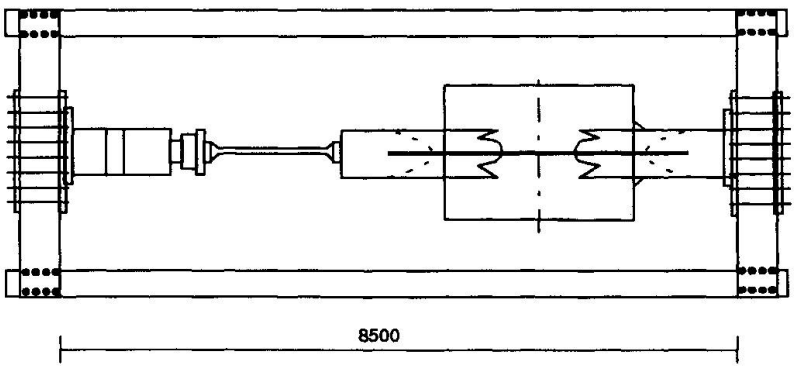

Figure 2 Test rig

2.2 Crack initiation and growth

Fracture surface examinations showed that multiple cracks developed along the welds during the first stage of crack growth, i.e. fatigue cracks were initiated at various sites along the weld toe before joining into one single crack (crack coalescence). Typically crack coalescence occurred at a crack depth of 3 mm.

Cracks at the brace column weld (Pos. 1) had a two stage development as shown in Fig. 3. In stage 1, a semi-elliptical surface crack generated from multiple crack initiation was growing in the through thickness direction of the brace wall. Typically 5-7 crack initiation sites were observed in the hot spot region. The surface crack length at the stage of through thickness crack penetration was typically 5-6 times the wall thickness. The through thickness crack was detected by leakage of white spirit.

Once the crack front had penetrated the wall thickness, the crack grew as a three-fronted crack in the brace and in the internal stiffening. Due to significant local bending at the brace/column weld, the growth rate in the brace wall at the external surface significantly exceeded the growth at the internal surface. Crack growth into the internal stiffening was significantly delayed by the root gap of the fillet weld, due to the re-initiation period.

At the end of testing, one of the brace/column weld cracks had reached a surface length of 285 mm. The crack length into the internal stiffening was only 40 mm. The number of cycles applied at this stage exceeded life to through thickness crack penetration by a factor 2.2 approximately. Thus, significant residual life remained after through thickness crack growth at the brace/column weld.

Cracks causing failure at the gusset welds (Pos. 2) went through the same stages of crack growth as observed with the brace/column welds, cf. Fig. 4. In stage 1, however, the occurrence of multiple crack initiation was limited by the length of the gusset end weld. Typically 2-3 cracks developed. Moreover, after crack coalescence, subsequent crack growth in the width direction was delayed by the absence of the notch effect of the weld. For these reasons, the surface crack length at the end of stage 1 was somewhat smaller than observed with the brace/-column welds, being typically 3-4 times the wall thickness.

In stage 2, the transition into a through-thickness crack in the brace occurred within a small number of cycles. For reasons outlined above, crack growth into the internal stiffening was significantly delayed.

At the end of testing, one of the gusset weld cracks had reached a surface crack length of 320 mm. The number of cycles applied at this stage exceeded life to through thickness crack penetration by a factor 1.6 approximately. With reference to similar data obtained with the brace/column welds (Pos. 1) this is a significant reduction in residual life. In average, the growth of through thickness cracks at Pos. 2 was twice as large as the growth observed at Pos. 1. The total effect of the gusset was to increase the life to through thickness penetration, and to reduce residual fatigue life in stage 2 almost correspondingly.

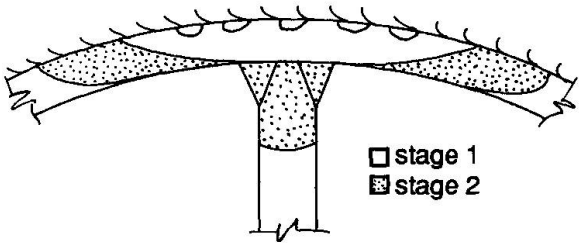

Figure 3 Stages of crack growth at brace/column welds

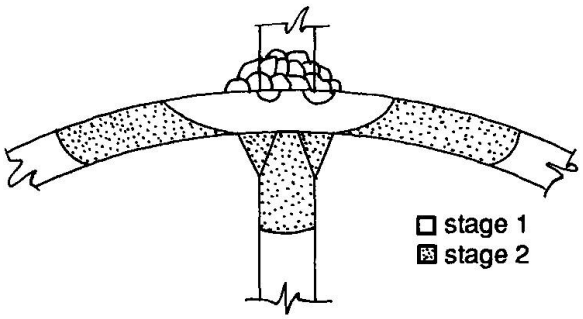

Figure 4 Stages of crack growth at external stiffener details

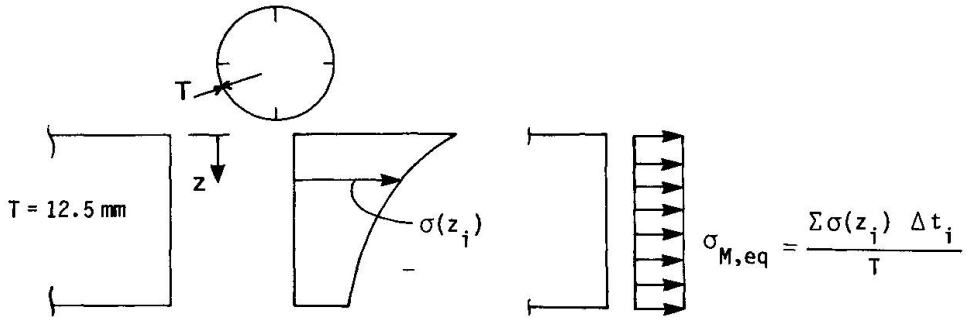

Figure 5

3. FRACTURE MECHANICS MODELS

Fatigue life of welded joints has been shown to consist mainly of crack growth from pre-existing crack-like defects in the weld toe region [2,3]. In the present study only the crack growth stage was considered, i.e. a possible crack initiation stage was neglected.

An in-house computer program, CALPRED [7], was used for the fracture mechanics calculations. Crack growth was assumed to follow the Paris-Erdogan type crack growth law

$$\frac{da}{dN} = C(\Delta K)^m \qquad (1)$$

Crack growth of surface cracks was calculated in two directions - through thickness at the deepest point and in the surface direction. A step-wise integration of crack growth with updating of the aspect ratio a/2c was applied. Numerical tests showed that the procedure had satisfactory accuracy.

The parameters C and m of Eqn. (1) were assumed to be equal at all positions along the crack front. Tests with simple specimens with semi-elliptical cracks, however, have shown that the crack growth rate tends to be lower at the free surface, most probably due to the larger plastic zone at this position [5]. This was taken into account by a reduction of the stress intensity factor K at the free surface by a factor $F_c = 0.91$, accounting for the plane stress condition at the surface.

The values of C and m were assumed as $C = 4.9 \cdot 10^{-12}$ [MPa $m^{1/2}$, m], $m = 3.1$. These values fall within the scatterband of crack growth data for various structural steels [6] and are recommended for fracture mechanics analysis of crack growth in welded steel structures [4].

In the analyses of the semi-elliptical cracks, i.e. stage I in Figs 3 and 4, the stress intensity factor determined by Newman and Raju [8] was applied.

$$K = (\sigma_M + H\sigma_B)\sqrt{(\frac{\pi a}{Q})} \cdot F^{N-R} \qquad (2)$$

The membrane and bendings stresses were obtained from shell analysis of the specimens [9]. Eqn. (2) does not account for the local stress concentration and corresponding nonlinear through thickness stress distribution at the weld toe. This was included in the following manner. In the deepest point of the crack, Eqn. (2) was used to account for the global stress concentration of the joint. The additional notch stress distribution due to the local stress concentration from the weld geometry was accounted for by the influence function method (point load model) proposed by Albrecht and Yamada [10] and developed further by Engesvik [11]. This leads to the resulting K in the deepest point.

$$K_{tot} = (\sigma_M + H\sigma_b)\sqrt{(\frac{\pi a}{Q})} \cdot F^{N-R} + \alpha_M \sigma_M \sqrt{(\pi a)} \cdot F^{A-Y} + \alpha_B \sigma_B \sqrt{(\pi a)} \cdot F^{A-Y} \qquad (3)$$

$$\alpha_M = SCF_{M,weld}^{-1}$$

$F^{A-Y} = F_S \cdot F_T \cdot F_W \cdot F_E \cdot F_G$, corrections for geometry of crack, specimen, stress distribution

In the surface width direction, the Newman-Raju solution was calculated using the stresses at the crack tip location, including the global stress variation from shell analysis, and the local stress concentration of the weld. The local stress distribution in the weld toe region was determined by plane FEM analyses with very small elements distributed through the thickness [9]. The parameters describing the weld geometry, i.e. throat angle θ and toe radius ρ, were obtained by measurements on the specimens.

For the analysis of through cracks, i.e. stage 2 in Figs 3 and 4, the solution for K for through cracks with a straight crack front was employed [12]. The loading was, however, separated in a nominal membrane stress which was constant around the circumference and a varying membrane stress distribution around the circumference due to reduction in stresses when the crack grew away from the stress concentration of the stiffener.

$$K_{tot} = \sigma_M \sqrt{(\pi a)} + \alpha_{eq} \sigma_M \sqrt{(\pi a)} \cdot F_{G,through} \qquad (4)$$

In the model the brace was assumed to be a plate of large width, hence the finite width correction F_W was negligible. The K-solution given in Eqn. (4) is limited to membrane stress. At the brace/column intersection, there were also shell bending and weld notch stresses, cf. Fig. 5. The distribution of these stresses was calculated around the circumference of the brace. An equivalent membrane stress, which at each location around the circumference would give the same cross sectional force as the total stress distribution, was calculated and applied in Eqn. (4), see Fig. 5.

4. FRACTURE MECHANICS ANALYSIS AND DISCUSSION

4.1 Analysis of growth of semi-elliptical cracks

One of the major problems in fracture mechanics analysis of fatigue cracks initiating at weld toes, is the assessment of the size and shape of initial cracks. It has been demonstrated that crack-like defects in the weld toe region is an inherent feature of welds produced by conventional welding processes. These defects are non-metallic slag intrusions along the fusion line, formed when the metal is melted or pasty during welding. The size and shape of the defects have been found to be quite random, with typical depths in the range 0.05-0.4 mm [2,3].

In Fig. 6 are shown experimental crack shape data for brace/column weld cracks (Pos. 1) with fracture mechanics predictions assuming an initial crack $a_0/2c_0$ = 0.4/0.8. Similar data obtained for the gusset cracks (Pos. 2) are shown in Fig. 7.

In the analysis, growth of a single crack was modelled, i.e. the multiple crack initiation and crack coalesence effects were not taken into account. These effects were particularly pronounced at the brace/column weld (Fig. 6). For long cracks, the computational model and the test data appear to be converging towards an aspect ratio a/2c in the range 0.2-0.3. In the initial stages of crack growth, however, there is a significant discrepancy.

The data from Pos. 2 (Fig. 7) were less affected by multiple initiation, and there is an overall agreement between analysis and experiments. However, the scatter in experimental data makes conclusions uncertain.

In Figs 8 og 9 are shown crack growth data and analysis for through thickness crack growth at the two positions of the model. With assumptions of an initial crack size within what has been reported for manual welds [2, 3], there is an overall agreement between tests and analysis. It is noted that at Pos. 1, the predictions tend to underestimate crack growth, i.e. good fit is obtained if a relatively large initial defect size to assumed. The reason for this is most probably the effects of crack coalescence, Fig. 6.

In similar analyses, using a forcing function for a/2c in order to simulate crack coalescence, very good correlation between tests and analysis has been reported [11, 13]. However, in order to apply a forcing function, the experimental data for a/2c need to be known a priory, making the method less of a predictive nature. Also shown in Fig. 8 is the effect of omitting the variation in stress around the circumference of the weld (dotted line), i.e. performing the analysis on the basis of the stress at Pos. 1.

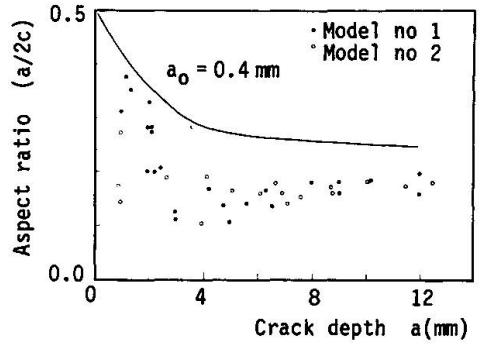

Figure 6 Crack shape data for part-through cracks at brace/column weld (Position ①, cf. Fig.1)

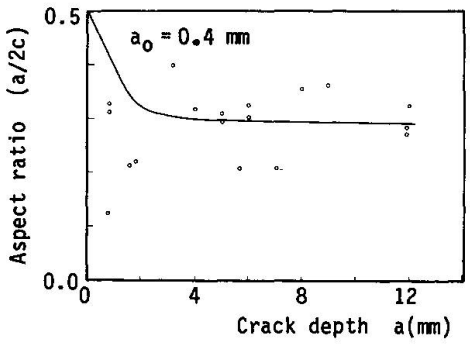

Figure 7 Crack shape data for part-through cracks at external stiffener welds (Position ②, cf. Fig.1)

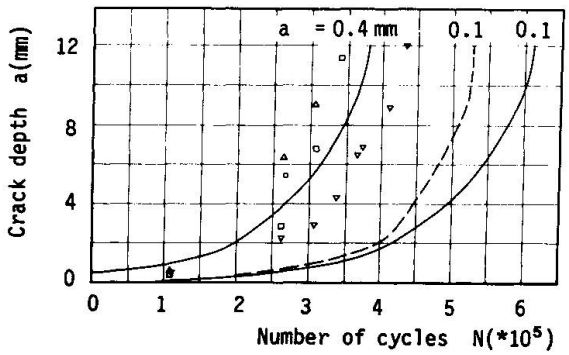

Figure 8 Crack growth data for part-through cracks, position ①, model no. 2

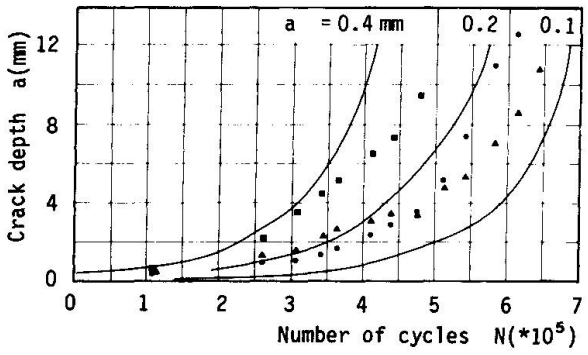

Figure 9 Crack growth data for part-through cracks, position ②, cf. Fig.1

4.2 Analysis of through thickness cracks

In Fig. 10 the development of through cracks at the brace/column weld is shown. The transition from a semi-elliptical crack to a through crack was modelled by simply taking a straight crack front with a width equal to the surface width of the semi-elliptical crack at the stage of through thickness penetration. As seen from Fig. 3 the crack front is far from being straight due to the significant bending and notch stresses.

Two values for the initial through thickness crack size were employed. The top curve in Fig. 10 was obtained with the measured mean value of the width of the three cracks. The lower curve was obtained with the width of the computed crack, i.e. a computational model covering both stages of crack growth. This value was smaller than the measured ones due to an overestimated a/2c - ratio in the calculation of semi-elliptical crack growth (Fig. 6). The figure shows that for cracks larger than ~ 150 mm, the computed crack growth rate is too high compared to the test results. This may be explained by the stress redistribution from the brace wall and into the stiffener. Since the computed results are based on the stresses in the original uncracked geometry, the redistribution is not accounted for.

In Fig. 11 the crack growth results of through thickness cracks at end of the gusset (Pos. 2) are shown. In this case the initial crack width obtained from the width of the semi-elliptical crack at through thickness corresponded closely with the test results. The gusset weld and internal stiffener had only a local influence on the crack growth at this position. For the through thickness crack stage, the membrane stress in the chord wall was dominating, and the uncertainty in modelling Eqn. 4 was much less than in the case of the brace/column weld. Still, there is a significant difference between the computed and the measured crack developments, underlining the assumption that load shedding effects are important.

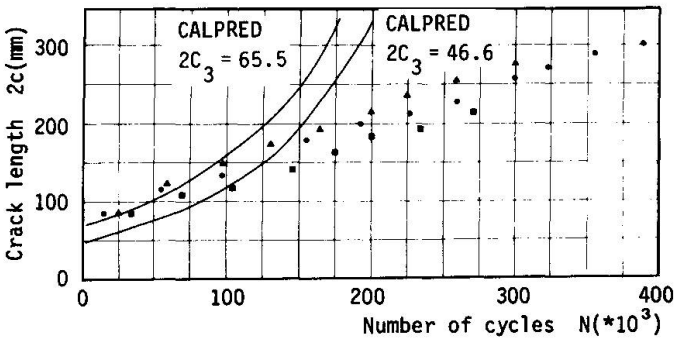

Figure 10 Crack growth data for through-thickness cracks, position ① , cf. Fig.1

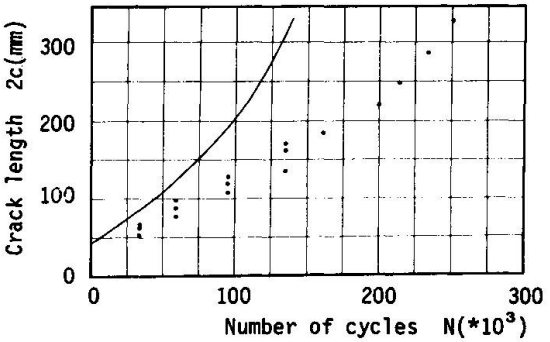

Figure 11 Crack growth data for through thickness cracks, position ② , cf. Fig.1

5. CONCLUSIONS

Fatigue crack growth in simplified but realistic models of brace/column connections typical of semi-submersible rigs was studied. A fracture mechanics model was established in order to predict the observed crack growth behaviour. The following observations were made,

- Significant multiple crack initiation occurred at hot spot regions of the brace/column welds. Crack coalescence occurred at a typical crack depth of 3 mm, introducing a significant change in the crack shape development.
- For surface cracks, a two-parameter fracture mechanics model calculating crack shape development was established. Without taking crack coalescence into account, the model gave results in reasonable agreement with test data.
- At external gusset welds, multiple crack initiation was less pronounced. In this case, good agreement between predicted and experimental data was obtained for through thickness crack growth.

- After through thickness penetration, a significant residual fatigue life remained before catastrophic crack growth took place. For the brace/column weld, the total life was as much as 2.2 times the through thickness life. For the external gusset, the same factor was 1.6. Total life for both details was approximately the same.
- The predicted growth of through thickness cracks tended to underestimate residual life, probably due to load shedding effects which were not accounted for.

6. REFERENCES

1. EIDE, O.I. and BERGE, S.: Fatigue Capacity and Crack Growth in Stiffened Tubular Joints. SINTEF Report STF71 A89011, 1989. Also OMAE 1990.

2. SIGNES, E.G. et al.: Factors Affecting Fatigue Strength of Welded High Strength Steels. British Welding Journal, March 1967.

3. WATKINSON, F. et al.: The Fatigue Strength of Welded Joints in High Strength Steels and Methods for its Improvement. Proceeding Conference on Fatigue of Welded Structures, Brighton 1970.

4. DnV Classification Note 30.2: Fatigue Strength Analysis for Mobile Offshore Units, 1984.

5. RAJU, I.S. and NEWMAN, J.C.: An Empirical Stress Intensity Factor Equation for the Surface Crack. Eng. Fract. Mech., Vol. 15, pp. 185-192, 1981.

6. ECSC Conference on Steel in Marine Structures, Institut de Recherches de la Siderurgie Francaise, Paris, 1981.

7. SKALLERUD, B.: CALPRED, Computer Aided Life Predictions. SINTEF Report STF71 A89055, 1989.

8. NEWMAN, J.C. and RAJU, I.S.: Stress Intensity Factor Equations for Cracks in Three-Dimensional Finite Bodies Subjected to Tension and Bending Loads. Chpt. 9 in Computational Methods in the Mechanics of Fracture, Ed. S.N. Atluri, Elsevier Science Publ. B.V., 1986.

9. BRODTKORB, B.B.: Stress Analysis of a Tubular Joint with Internal Stiffening. SINTEF Report STF71 A89006, 1989.

10. ALBRECHT, P., YAMADA, K.: Rapid Calculation of Stress Intensity Factors. Jour. Struct. Div., ASCE, Vol. 103, pp. 377-389, 1977.

11 ENGESVIK, K.: Analysis of Uncertainties in the Fatigue Capacity of Welded Joints. Dr.ing. Thesis, The Norwegian Institute of Technology, Division of Marine Structures, 1982.

12. TADA, H., PARIS, P.C., IRWIN, G.R.: The Stress Analysis of Cracks, Handbook. Del Research Corp., 1985.

13. EIDE, O.I. and BERGE, S.: Fracture Mechanics Analysis of Welded Girders in Fatigue. Int. Conf. Fatigue of Welded Constructions, Brighton, 1987.